Cleaner Engineering and Technology 14 (2023) 100640

Contents lists available at ScienceDirect

Cleaner Engineering and Technology

journal homepage: www.sciencedirect.com/journal/cleaner-engineering-and-technology

Thermodynamic analysis of bio-oil model compounds to light hydrocarbon

Muhammad Zakwan Najohan [a], Zaki Yamani Zakaria [a,b,*], Mazura Jusoh [a,c], Anas Abdulqader Alshaikh [a], Muhammad Tahir [d], Didi Dwi Anggoro [e]

[a] Faculty of Chemical and Energy Engineering, Universiti Teknologi Malaysia, 81310, Skudai, Johor, Malaysia
[b] Centre for Engineering Education, Universiti Teknologi Malaysia, 81310, Skudai, Johor, Malaysia
[c] Institute of Biotechnology Development, Universiti Teknologi Malaysia, 81310, Skudai, Johor, Malaysia
[d] Chemical and Petroleum Engineering Department, United Arab Emirates University, 15551, Al Ain, United Arab Emirates
[e] Department of Chemical Engineering, Faculty of Engineering Diponegoro University, Indonesia

ARTICLE INFO

Keywords:
Bio-oil
Thermodynamic modeling
Light hydrocarbons
Cracking
Model compound mixture

ABSTRACT

The present work uses the total Gibbs free energy minimization approach to analyze the thermodynamic equilibrium analysis of bio-oil model compounds to light hydrocarbons. A mixture of model compounds was subjected to co-cracking with methanol and ethanol, and at a range of temperatures (300–1200 °C) and pressures (1–50 bars), the equilibrium compositions were calculated as a function of the hydroxypropanone-acetic acid-ethyl acetate/methanol ratio (HAEM) and the hydroxypropanone-acetic acid-ethyl acetate/ethanol ratio (HAEE). Possible reactions were analyzed, revealing that methane is the predominant product, followed by hydrogen, carbon monoxide, carbon dioxide, and propionic acid. The production of light hydrocarbons, including ethylene, ethane, propylene, and propane, was minimal. Notably, the co-reactant ethanol (HAEE 1:12) in the co-cracking of bio-oil model compounds demonstrated a significant effect on the production of methane, ethylene, and propylene at 1 bar pressure and 300 °C (for methane production) and 1200 °C (for ethylene and propylene production).

1. Introduction

Biomass is known as organic matter that comes from living organisms such as wood, crops, seaweed, and animal waste. According to its chemical composition, biomass can be generally categorized into first-generation biomass (e.g., sugars and vegetable oils), second-generation biomass (e.g., rice husk and wood chips), and third-generation biomass (e.g., microalgae and macroalgae) (Zhang et al., 2021). Biomass mainly consists of cellulose, hemicellulose, lignin, protein, or lipid. These organic materials can be converted via either biochemical or thermochemical conversion approaches. Thermochemical conversion on biomass consists of hydrothermal liquefaction, combustion, pyrolysis, and gasification (Hu and Gholizadeh, 2020). Bio-oil is among the higher value-added product obtained from the thermochemical conversion.

Bio-oil is an alternative renewable energy source used in the production of chemicals or as a renewable liquid fuel. It is a clean fuel, zero-carbon fuel, less harmful gas emission, and applicable for boilers and burners after modifying the existing units (Lehto et al., 2018; Ritchie and Roser, 2020). Despite the environmental benefits of bio-oils in reducing CO_2 emissions, their unsuitable properties, including high oxygen content (40–50 wt%), low levels of carbon and hydrogen, an acidic pH, high levels of instability and immiscibility, and low LHV, make them inappropriate as drop-in fuels (Bertero et al., 2012; Kumar et al., 2020; Lawal and Farrauto, 2013; Londoño-Pulgarin et al., 2021).

Comprising water and intricate oxygen-rich organic compounds, bio-oil includes a range of phenols, ketones, aldehydes, ethers, organic acids, alcohols, and esters (Hu and Gholizadeh, 2020; Lawal and Farrauto, 2013; Ritchie and Roser, 2020). The pyrolysis conditions that are employed and the kind of biomass that is used determine the content of the bio-oil (Huang et al., 2013; Rodrigues et al., 2020). Model compounds are extensively researched because of their clearly defined chemical structures due to the variety and complexity of bio-oils (Sahebdelfar and Ravanchi, 2017). Since bio-oil contains various chemical compounds, some chemicals can function as a potential source to produce other valuable products, such as light hydrocarbon (as energy). Since there are more than a hundred chemicals in a particular bio-oil compound, the most abundant ones available are

* Corresponding author. Faculty of Chemical and Energy Engineering, Universiti Teknologi Malaysia, 81310, Skudai, Johor, Malaysia.
E-mail address: zakiyamani@utm.my (Z.Y. Zakaria).

https://doi.org/10.1016/j.clet.2023.100640
Received 20 February 2023; Received in revised form 8 April 2023; Accepted 7 May 2023
Available online 8 May 2023

hydroxypropanone (Aziz et al., 2021), acetic acid (Liang et al., 2021), and ethyl acetate (Velayuthem et al., 2021) has been considered as the model compound, to represent bio-oil, in this study.

The model compound can be directly converted via a thermochemical conversion approach by employing cracking reaction to other products including light hydrocarbon, but it may not provide an attractive yield. This is primarily due to the low $(H/C)_{eff}$ ratio nature. To convert the model compound into precious light hydrocarbon, compounds with higher $(H/C)_{eff}$ ratios were used to raise the reactants' integral $(H/C)_{eff}$ ratio to improve the stability of the cracking process (Wang et al., 2015) in forming higher light hydrocarbons. Aliphatic alcohols are considered optimal co-reactants as they display an elevated $(H/C)_{eff}$ ratio of 2, ensuring steady conversion under comparable operating conditions. Consequently, methanol and ethanol, owing to their affordability and easy accessibility, are the most widely utilized alcohols (Wang et al., 2014). The utilization of a mixture of methanol/ethanol in conjunction with a bio-oil model compound blend to generate light hydrocarbons appears to be an interesting and potentially fruitful avenue for further investigation.

Performing experimental investigation for the co-cracking of the bio-oil model compound and methanol/ethanol could be substantially costly and consume a massive time (Velayuthem et al., 2021). The experiments could be better served as a verification step after a proper preliminary study is conducted. Hence, the examination of the product distribution for the co-cracking reaction in a given process necessitates a thermodynamic equilibrium analysis, as a preliminary investigation. By reducing the system's overall Gibbs free energy, the equilibrium distribution of the products is examined at a fixed temperature and pressure. Such analysis offers a useful manual for developing and designing processes (Sahebdelfar, 2017). It makes it possible to evaluate the viability of intricate chemical reaction systems and the impact of process factors on the equilibrium product composition. Furthermore, it assists in identifying the thermodynamically ideal operating conditions for targeted production (Dhanala et al., 2015). HSC Chemistry software is employed for thermodynamic modeling purposes. Owing to that, the objective of this research is to examine the thermodynamics of co-cracking bio-oil model compounds into light hydrocarbons. The effects of temperature, pressure, and feed ratio are investigated using the method of minimizing the total Gibbs free energy. Unlike the previous study, this investigation combined three top abundant chemicals contained in the complex bio-oil mixture (hydroxypropanone, acetic acid, and ethyl acetate) as an integrated model compound to better and more accurately represent bio-oil as a feedstock.

2. Methodology

2.1. Study objective and calculation conditions

The co-cracking process of the bio-oil model compound was analyzed thermodynamically by utilizing HSC Chemistry version 6.0 to minimize the total Gibbs energy. The investigation focused on three primary thermodynamic factors: temperature, pressure, and feed ratio. The bio-oil model compounds and methanol/ethanol were considered as the reactant. A 1 kmol feed was fixed for all reactants at the input. The operating temperature range was between 300 °C and 1200 °C with the operating pressure range between 1 and 50 bars. The molar ratio of HAEM (hydroxypropanone - acetic acid - ethyl acetate to methanol ratio) and HAEE (hydroxypropanone - acetic acid - ethyl acetate to ethanol ratio) were 1:12, 1:6, 1:3, 1:1 and 2:1.

By employing the Gibbs program, the equilibrium composition of the system can be determined based on a specific temperature, pressure, and feed composition. The program identifies the most stable combination of species and calculates the phase compositions where the system's Gibbs energy reaches its minimum while maintaining constant pressure and temperature and a fixed mass balance. Consequently, the input does not require any reaction equations. The HSC Chemistry software package's built-in databases were used to carry out material and energy balance calculations. It was assumed that the reaction products were in thermodynamic equilibrium upon exiting the reactor. The results showed that complete conversion (100%) of bio-oil and positive product yields were achieved in all the analyzed cases, indicating the viability of the bio-oil co-cracking process.

2.2. Gibbs free energy minimization

Balanced thermodynamic calculations of a complex reaction system often use the equilibrium constant technique, relaxation method, and Gibbs's free energy minimization approach to address the issues with phase and chemical equilibrium in a series of chemical reactions (Sahebdelfar, 2017). The Gibbs free energy minimization technique is regarded as one of these strategies that are most useful for finding out the equilibrium compositions of each component in a complicated system (Liu et al., 2019). This method is based on the concept that the total Gibbs free energy of the system equals the sum of the standard Gibbs free energies of all the pure components and the mixed system at equilibrium. The equation is presented below:

$$G^t = \sum_{i=1}^{N} n_i \overline{G}_i = \sum_{i=1}^{N} n_i \mu_i = \sum n_i \overline{G}_i^0 + RT \sum n_i \, ln \frac{\widehat{f}_i}{\widehat{f}_i^0} \quad (1)$$

A non-stoichiometric method was utilized to identify the system's chemical species' equilibrium composition. By minimizing the Gibbs free energy without having to select certain chemical processes or exactly estimate the starting equilibrium composition, convergence in computation was quickly obtained. The chemical species simply needed to be identified based on the possible reactions.

Temperature (T), pressure (P), and the number of moles of the N components in the system all affect the Gibbs free energy (G). The differential form of the Gibbs free energy can be expressed as follows:

$$dG = -SdT + VdP + \sum_{i=i}^{N} \mu_i dn_i \quad (2)$$

where n_i is the number of moles of each component in the system, V is the volume, S is the entropy, and μ_i is the appropriate chemical potential. When the system is operating under isobaric and isothermal conditions, the differential equation changes to:

$$dG = \sum_{i=i}^{N} \mu_i dn_i \quad (3)$$

Once the system attains equilibrium under the correct temperature and pressure, it is possible to directly employ Gibbs free energy minimization to establish the equilibrium composition of each component in the mixture. This approach involves setting equation (3) equal to zero, as at equilibrium, the system possesses the minimum Gibbs free energy.

3. Results and discussion

3.1. Equilibrium constant and probable reactions

A basic set of reactions was created to represent the thermodynamic conversion of hydroxypropanone, acetic acid, and ethyl acetate into light hydrocarbons to take into consideration the complexity of the assumed processes. Table 1 displays the potential reactions that may arise during the co-cracking process, while Fig. 1 shows the equilibrium constants of all supposed reactions as a function of temperature. According to the principles of thermodynamics, if the Gibbs free energy change of reaction (ΔGr) is negative, the reaction is considered spontaneous, while a positive ΔGr signifies that the reaction is thermodynamically restricted. It is important to note that the equilibrium constant (K) governs the extent of the reaction. At the point where K is significantly bigger than 1, altering the molar ratio of reactants will not shift the reaction to the other side. On the other hand, when K is close to 1, altering the molar ratio of the reactants significantly affects the product

Table 1
Possible reaction in co-cracking of acetic acid, hydroxypropanone, and ethyl acetate.

Reaction	Type of Reaction	Reaction	ΔH (kJ/mol)
R1	Thermal decomposition of acetic acid	$CH_3COOH \Leftrightarrow 2CO + 2H_2$	+213.70
R2	Thermal decomposition of acetic acid	$CH_3COOH \Leftrightarrow CH2CO + H_2O$	−33.50
R3	Thermal decomposition of acetic acid	$CH_3COOH \Leftrightarrow CH_4 + CO_2$	+16.19
R4	Thermal decomposition of hydroxypropanone	$C_3H_6O_2 \Leftrightarrow C_3H_4O + H_2O$	−32.43
R5	Thermal decomposition of hydroxypropanone	$C_3H_6O_2 \Leftrightarrow CO_2 + C_2H_6$	+107.19
R6	Thermal decomposition of ethyl acetate	$C_4H_8O_2 \Leftrightarrow CH_3COOH + C_2H_4$	+65.81
R7	Water gas shift reaction	$CO + H_2O \Leftrightarrow H_2 + CO_2$	−41.14
R8	Steam reforming of hydroxypropanone	$C_3H_6O_2 + 4H_2O \Leftrightarrow 7H_2 + 3CO_2$	−156.88
R9	Steam reforming of acetic acid	$CH_3COOH + 2H_2O \Leftrightarrow 4H_2 + 2CO_2$	+131.40
R10	Steam reforming of ethyl acetate	$C_4H_8O_2 + 6H_2O \Leftrightarrow 4CO_2 + 10H_2$	+322.20
R11	Methanation	$CO + 3H_2 \Leftrightarrow CH_4 + H_2O$	−206.10
R12	Methanation	$CO_2 + 4H_2 \Leftrightarrow CH_4 + 2H_2O$	−165.10
R13	Methanation	$2CO + 2H_2 \Leftrightarrow CH_4 + CO_2$	−247.30
R14	Oxidative coupling of methane	$3CH_4 + 4CO_2 \Leftrightarrow C_2H_6 + 5CO + 3H_2O$	+106.00
R15	Oxidative coupling of methane	$2CH_4 + 2CO_2 \Leftrightarrow C_2H_4 + 2CO + 2H_2O$	+284.00
R16	Dehydrogenation of ethane	$C_2H_6 \Leftrightarrow C_2H_4 + H_2$	+136.33
R17	Methane decomposition	$CH_4 \Leftrightarrow 2H_2 + C$	+74.52
R18	Boudouard reaction	$2CO \Leftrightarrow CO_2 + C$	−172.44
R19	Hydrogenation of CO_2	$CO_2 + 2H_2 \Leftrightarrow 2H_2O + C$	−90.16
R20	Hydrogenation of CO	$H_2 + CO \Leftrightarrow H_2O + C$	−131.30
R21	Dehydration to ketene	$CH_3COOH \Leftrightarrow CH_2CO + H_2O$	+144.40
R22	Ketonization	$2.5CH_3COOH \Leftrightarrow (CH_3)_2CO + 2H_2O + 2CO$	−156.53
R23	Ketene decomposition	$2CH_2CO \rightarrow C_2H_4 + 2CO$	−76.90
R24	Allene formation	$2CH_2CO \rightarrow C_3H_4 + CO_2$	−110.70
R25	Hydrocarboxylation of ethylene	$C_2H_4 + H_2O + CO \rightarrow CH_3CH_2COOH$	−171.59
R26	Hydrogenation of CO2	$CO_2 + 3H_2 \Leftrightarrow CH_3OH + H_2O$	−90.16
R27	MeOH dehydration	$2CH_3OH \Leftrightarrow CH_3OCH_3 + H_2O$	+23.33
R28	Hydrogenation of CO	$2CO + 4H_2 \Leftrightarrow CH_3OCH_3 + H_2O$	−131.30
R29	Dimethyl ether to Propylene	$1.5CH_3OCH_3 \Leftrightarrow C_3H_6 + 1.5H_2O$	+66.185
R30	Hydrogenation of Propylene	$C_3H_6 + H_2 \Leftrightarrow C_3H_8$	−124.22

distribution. If ΔGr is negative, a higher ln K value indicates that a spontaneous reaction is more likely to occur.

As shown in Fig. 1, certain chemical reactions are highly spontaneous at all temperatures studied, including the thermal decomposition of acetic acid (R1 and R3), thermal decomposition of hydroxypropanone (R5), steam reforming of acetic acid (R9), steam reforming of ethyl acetate (R10), ketonization (R22), ketene decomposition (R23), allene decomposition (R24), hydrocarboxylation of ethylene (R25), methanol dehydration (R27), and dimethyl ether to propylene reaction (R29). On the other hand, the oxidative coupling of methane (R15), methane decomposition (R17), Boudouard reaction (R18), hydrogenation of CO2 (R19 & R26), and hydrogenation of CO (R20 & R28) are limited within the whole investigated temperature. The reactions of thermal decomposition of hydroxypropanone (R4), thermal decomposition of ethyl acetate (R6), and dehydration to ketene (R21) are not feasible at lower temperatures (<700 °C) due to their large negative ln K values. Dehydrogenation of ethane and oxidative coupling of methane (OCM) (R14) require high temperatures (>800 °C) to occur, and the reactions of water

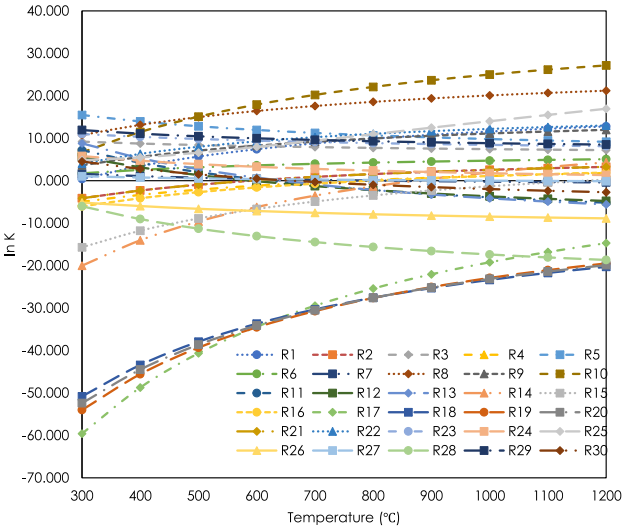

Fig. 1. Temperature dependence of the equilibrium constants of reactions involving co-cracking of hydroxypropanone-acetic acid-ethyl acetate at atmospheric pressure.

gas shift (R7), steam reforming of hydroxypropanone (R8), and hydrogenation of propylene (R30) are more likely to occur at lower temperatures (<700 °C). All the methanation reactions (R11, R12, and R13) are expected to occur at lesser temperatures (<700 °C) because of their positive ln K values, while at high temperatures (>700 °C), these reactions are limited by equilibrium.

3.2. Methane production

The co-cracking method's largest yield product in this study is methane. Methane formation was essential since it set the standard for the generation of light hydrocarbons. The moles of methane generated at various temperatures are shown in Fig. 2 along with HAEM. At lower temperatures, more methane was produced, but as the temperature rose, less methane was produced. The methanation process provides a clear explanation for this (R11, R12, and R13). Moreover, the amount of

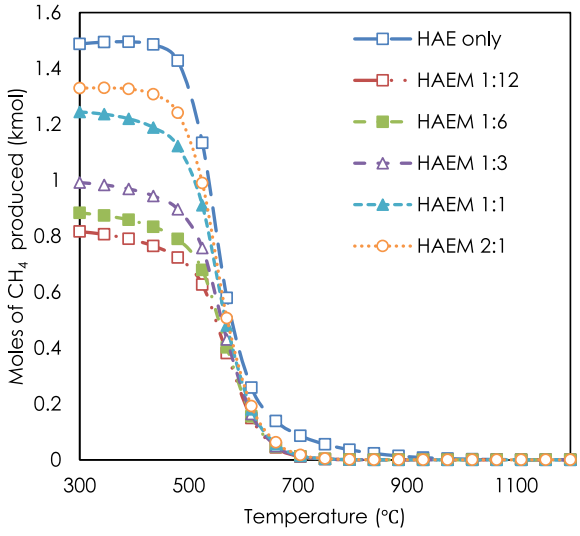

Fig. 2. Yield of CH_4 for different HAEM at 1 bar.

methane formed results from a spontaneous reaction of acetic acid's thermal breakdown (R3). The availability of methane is responsible to trigger the oxidative coupling of methane (OCM) reactions (R14 and R15), which results in the production of ethane and ethylene, respectively, along with carbon monoxide and water. In this case, methane will dissociate and form a very reactive methyl radical and be coupled between them to form C_2 products. From Fig. 2, the hydroxypropanone - acetic acid - ethyl acetate (HAE) has the highest yield of methane compared to HAEM. It could be seen that HAE can produce nearly twice the feed amount, 1 kmol.

Meanwhile, from Fig. 3, HAEE (HAEE = 1:12) has the highest yield of methane. It could be observed that HAEE has a significant effect starting at 500 °C on the production of methane. It can be deduced that HAEE did have a significant effect on the production of methane. The higher the ethanol ratio, the higher the formation of methane. The effect of both temperature and pressure for HAEM 2:1 and HAEE 2:1 was further analyzed toward the production of methane. From Figs. 4 and 5, it can be observed that lower pressure and lower temperature of the reaction produce higher methane yield. Therefore, the reaction parameters must be controlled at a suitable lower range temperature and pressure to obtain a higher yield of methane can be achieved.

3.3. Ethane formation

The amount of ethane moles formed at various HAEM/HAEE ratios, temperatures (300–1200 °C), and 1 bar are shown in Figs. 6 and 7. Thermal decomposition of hydroxypropanone reaction (R5) was one of the reactions responsible for the formation of ethane (apart from OCM). As can be observed from Figs. 6 and 7, the number of moles of ethane initially decreased with temperature. Moles of ethane went through a maximum of around 300 °C but decreased at higher temperatures as dehydrogenation of ethane (R16) proceeded, thus consuming ethane to form ethylene. HAEM minimizes the production of ethane within the studied parameter. However, the number of moles of ethane with HAEE initially increased in small amounts at a temperature (>900 °C). It could be observed that HAEE has a significant effect starting with the production of ethane. The production of water, hydrogen, carbon monoxide, and carbon dioxide was substantially more than the equilibrium moles of ethane. The production of ethane was reduced by the equilibrium constraint that R14 encountered. More significantly, methane can activate the oxidative coupling of methane reactions (R14 and R15), which will result in the production of ethane and ethylene, respectively, in addition to carbon monoxide and water.

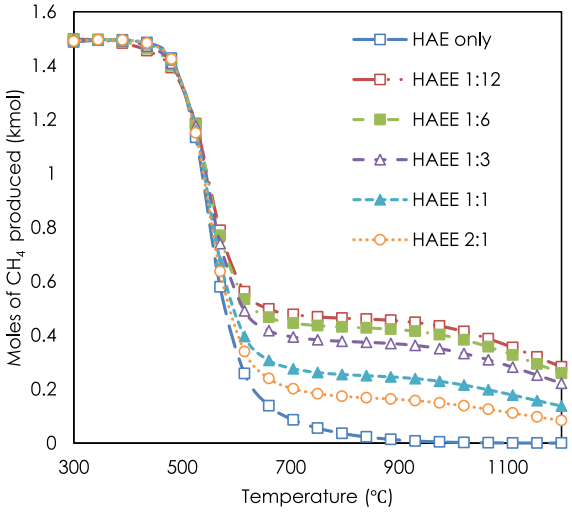

Fig. 3. Yield of CH_4 for different HAEE at 1 bar.

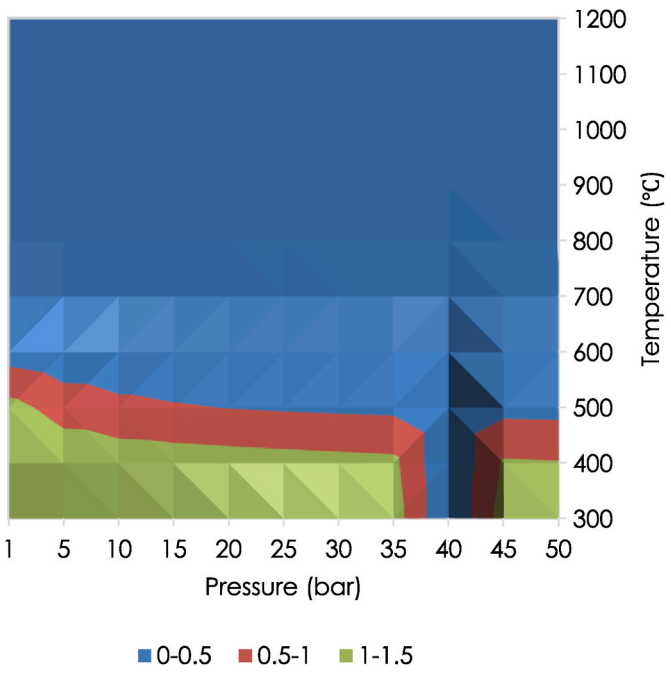

Fig. 4. Contour plot of methane formation (in kmol) as a function of pressure and temperature for HAEM 2:1.

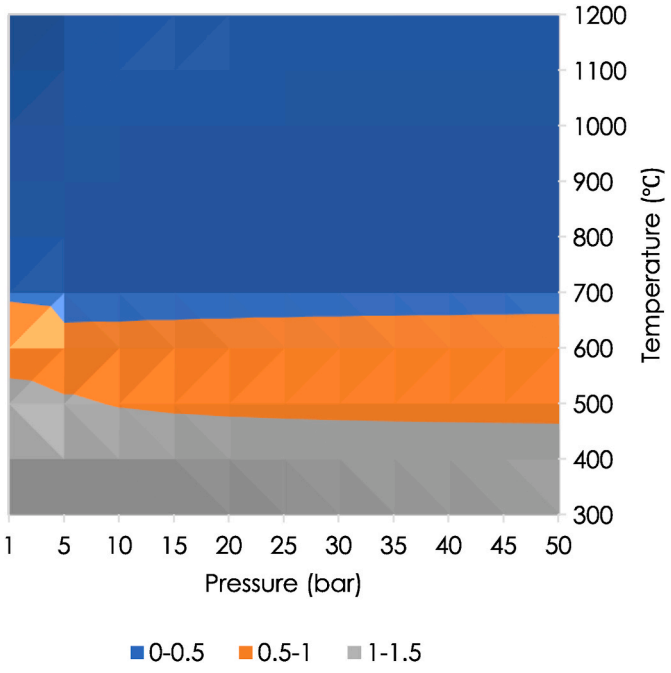

Fig. 5. Contour plot of methane formation (in kmol) as a function of pressure and temperature for HAEE 1:12.

The effect of both temperature and pressure for HAEM 2:1 and HAEE 2:1 was further analyzed toward the production of ethane. From Fig. 8, it can be observed that HAEM 2:1 produce higher ethane at higher pressure (35–45 bars) and higher temperature (650–1200 °C), which is interesting, considering the odd temperature-pressure combination. However, HAEE 2:1 as illustrated in Fig. 9, conveys a different outcome. Ethane is produced more at higher pressure (15–50 bars) and lower temperature range (300 °C) of the reaction. Therefore, the reaction parameters must be controlled at a suitable range to obtain a higher yield of ethane can be achieved.

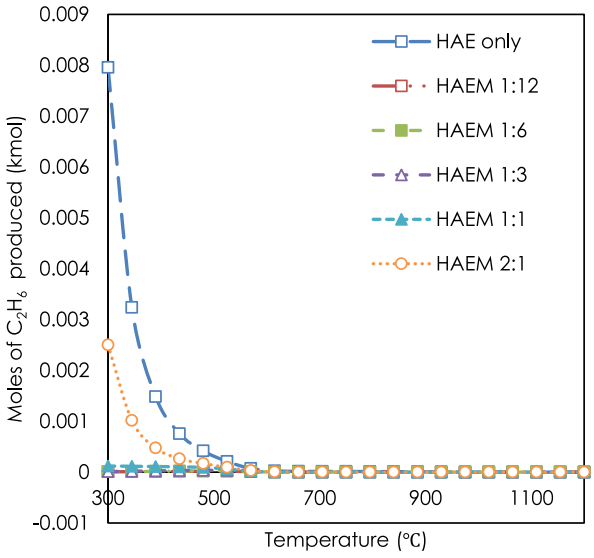

Fig. 6. Yield of C_2H_6 for different HAEM at 1 bar.

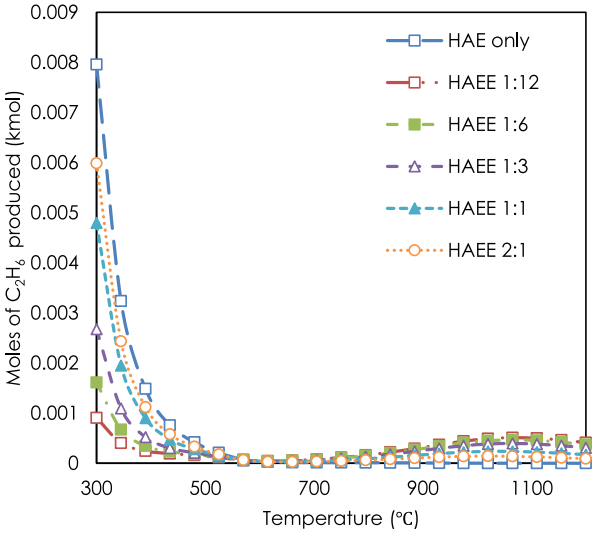

Fig. 7. Yield of C_2H_6 for different HAEE at 1 bar.

3.4. Ethylene formation

The amount of ethylene moles formed at diverse temperatures and various HAEM/HAEE ratios at 1 bar pressure are illustrated in Figs. 10 and 11. The amount of ethylene produced via HAEM is comparatively inferior to HAEE. As can be observed in Fig. 11, the moles of ethylene began to increase at 800 °C with the influence of HAEE. It then reached its maximum production at a high temperature of around 1200 °C. The production levels of ethylene were similar to those of ethane, suggesting that dehydrogenation of ethane (R16) at temperatures (>800 °C) predominantly boosted the production of ethylene, whereas R15 was subject to equilibrium limitations. The presence of methane could initiate the oxidative coupling of methane reaction (R14 and R15), which generated ethane and ethylene, along with carbon monoxide and water. However, HAEM had no impact on the production of ethylene.

The effect of both temperature and pressure for HAEM 2:1 and HAEE 1:12 was further analyzed toward the production of ethylene. From

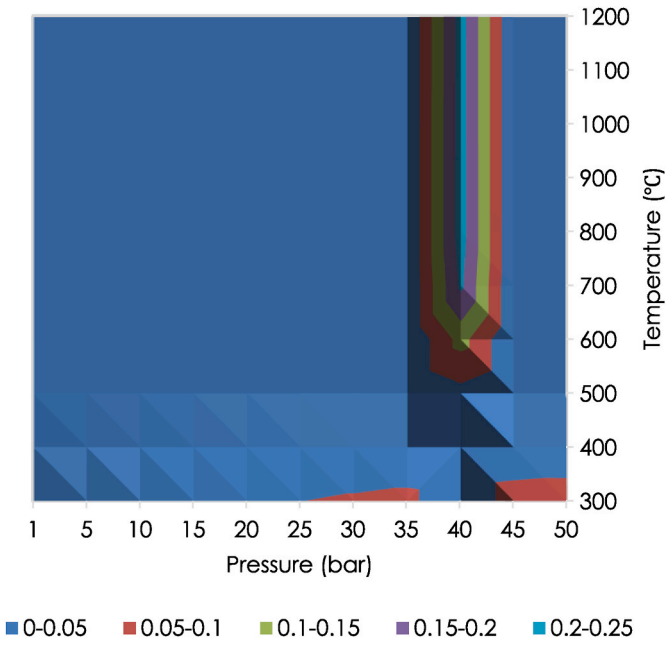

Fig. 8. Contour plot of ethane formation (in kmol) as a function of pressure and temperature for HAEM 2:1.

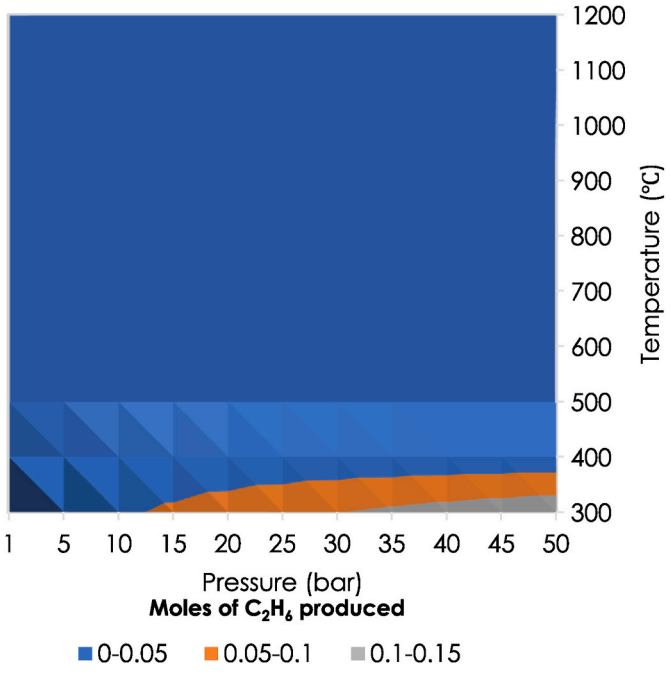

Fig. 9. Contour plot of ethane formation (in kmol) as a function of pressure and temperature for HAEE 2:1.

Fig. 12, it can be observed that HAEM 2:1 produce higher ethylene at a combination of higher pressure (35–45 bars) and lower temperature (300–400 °C). However, for HAEE 2:1 as illustrated in Fig. 13, it can be observed that lower pressure (1–5 bars) and higher temperature (1100–1200 °C) of the reaction produce higher ethylene yield. Therefore, the reaction parameters must be controlled at a suitable range to obtain a higher yield of ethylene can be achieved.

3.5. Hydrogen production

In the co-cracking process of bio-oil model compounds, hydrogen is

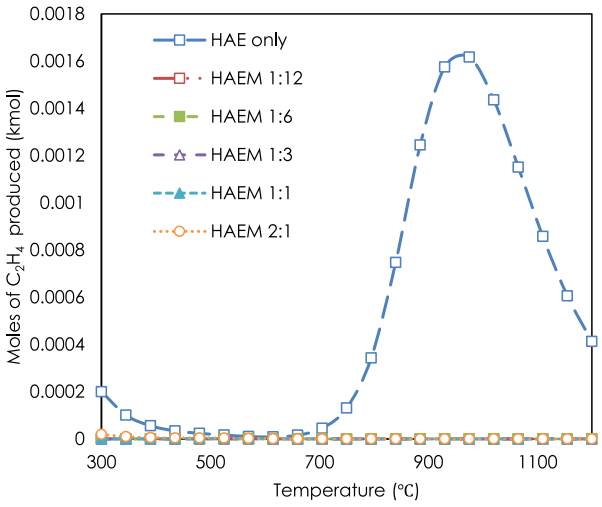

Fig. 10. Yield of C_2H_4 for different HAEM at 1 bar.

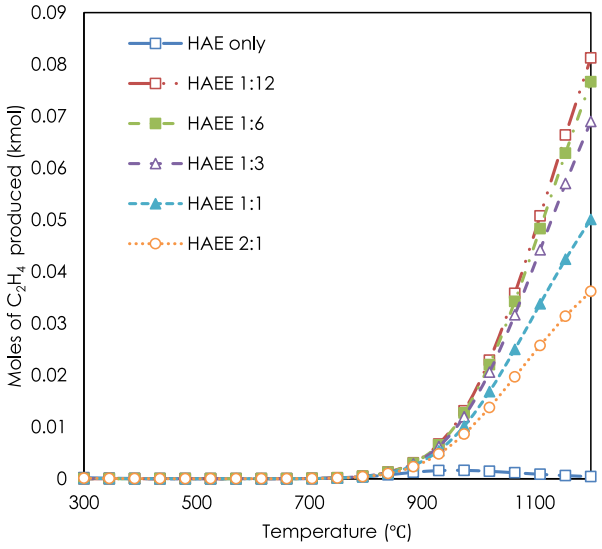

Fig. 11. Yield of C_2H_4 for different HAEE at 1 bar.

consistently the primary product. Figs. 14 and 15 illustrate the impact of HAEM/HAEE on hydrogen production at different process temperatures and 1 bar pressure. As depicted in the figures, increasing the temperature led to a gradual rise in hydrogen production until it reached its peak, after which it started to level off and decline. The HAEM/HAEE did have a significant effect on the amount of hydrogen produced. The thermal decomposition of acetic acid (R1) and the water gas shift reaction (R7) were responsible for the initial surge in hydrogen production, while methanation reactions (R11, R12, and R13) were unlikely to consume the hydrogen as they only occurred at lower temperatures. At high temperatures, the number of moles of hydrogen decreased with carbon dioxide while the moles of carbon monoxide and water gradually increased.

3.6. Carbon monoxide production

The relationship between temperature, HAEM/HAEE, and the production of carbon monoxide from co-cracking bio-oil model compounds are shown in Figs. 16 and 17. The results indicated that HAEM/HAEE

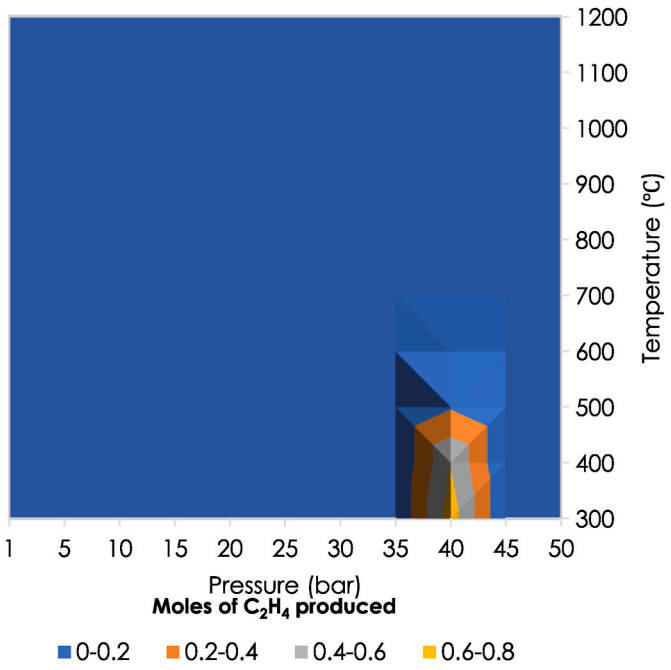

Fig. 12. Contour plot of ethylene formation (in kmol) as a function of pressure and temperature for HAEM 2:1.

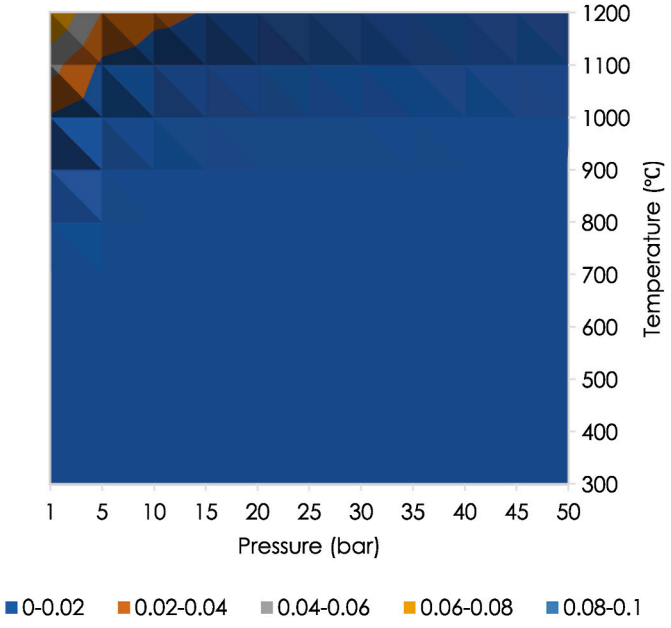

Fig. 13. Contour plot of ethylene formation (in kmol) as a function of pressure and temperature for HAEE 1:12.

had a significant impact on reducing carbon monoxide production, particularly at temperatures (<700 °C). At constant pressure and increasing HAEM/HAEE concentration, the production of carbon monoxide was highest between the temperature range of 500 °C–600 °C. The production of carbon monoxide was attributed to the thermal decomposition of acetic acid (R1), ketene decomposition (R23), and ketonization (R22).

3.7. Carbon production

The formation of carbon during the co-cracking process is undesirable because it deactivates the catalyst and increases pressure drop in

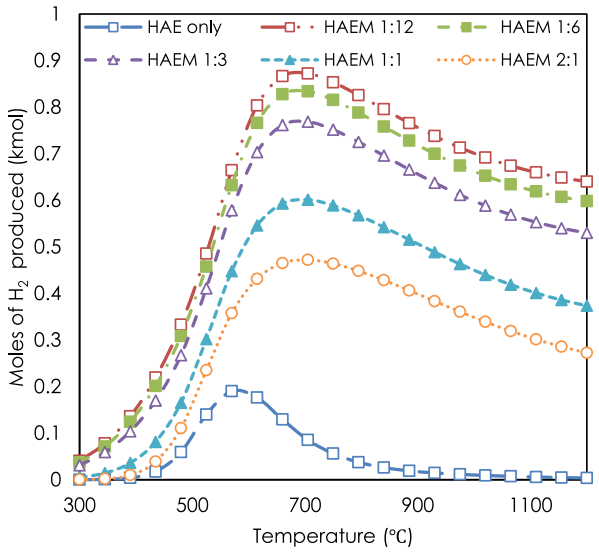

Fig. 14. Yield of H_2 for different HAEM at 1 bar.

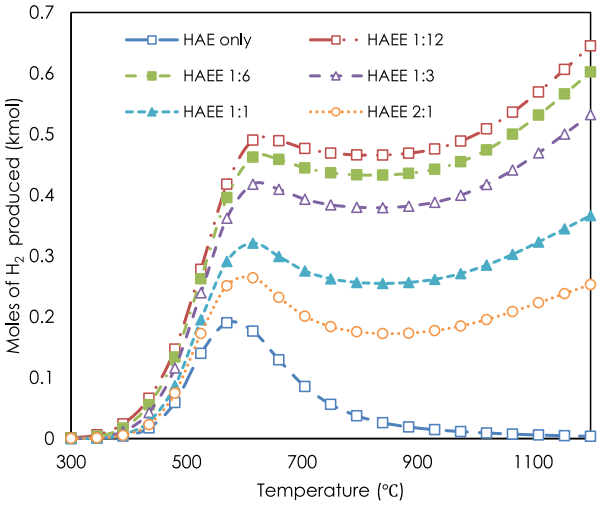

Fig. 15. Yield of H_2 for different HAEE at 1 bar.

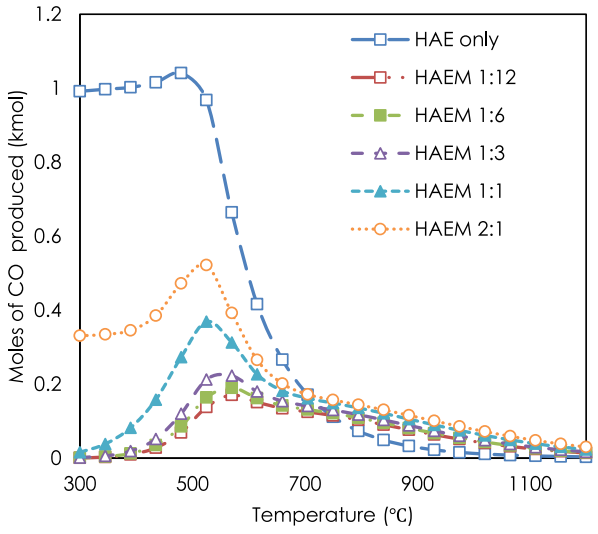

Fig. 16. Yield of CO for different HAEM at 1 bar.

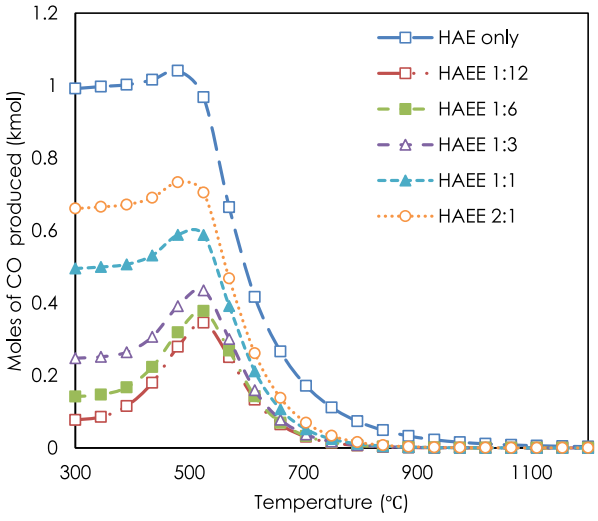

Fig. 17. Yield of CO for different HAEE at 1 bar.

reactors. Figs. 18 and 19 illustrate the production of carbon at varying temperatures and HAEM/HAEE concentrations. It was observed that the production of carbon on HAE only began to increase at around 1100 °C. The low production of carbon was attributed to the nonspontaneous reactions of R17, R18, R19, and R20. The formation of carbon through methane decomposition (R17), the Boudouard reaction (R18), hydrogenation of carbon dioxide (R19), and hydrogenation of carbon monoxide (R20) were strongly nonspontaneous at any temperature within the studied parameter. Therefore, there may be another reaction that produces carbon at high temperatures (1100 °C).

4. Conclusion

The effect of HAEM and HAEE for the production of light hydrocarbons at 300–1200 °C and 1 bar pressure has been studied using thermodynamic analysis of bio-oil model compounds on the co-cracking process. Additionally, the impact of changing pressure was tested to determine how it affected product yield. Thermodynamic equilibrium calculations reveal favourable yield for methane, propanoic acid, carbon dioxide, and syngas production. It can be observed that HAEM/HAEE as feedstock can maximize several productions of light hydrocarbon. To summarize, it could be seen that ethanol as a co-reactant (HAEE 1:12) in the co-cracking of bio-oil models compound has a significant effect on methane, ethylene, and propylene production at pressure 1 bar with the temperature 300 °C (methane production) and 1200 °C (ethylene and propylene production). The finding helps provide a better process parameter range to escalate this investigation to a newer dimension of thermodynamic study for further optimization work within this area, and also eventually verified by experimental work, and thus further it to future reaction kinetics and reaction mechanism study.

Declaration of competing interest

The authors declare that they have no known competing financial interests or personal relationships that could have appeared to influence the work reported in this paper.

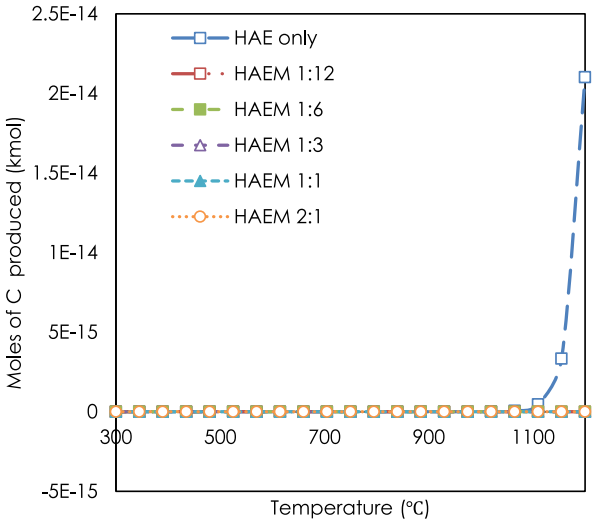

Fig. 18. Yield of C for different HAEM at 1 bar.

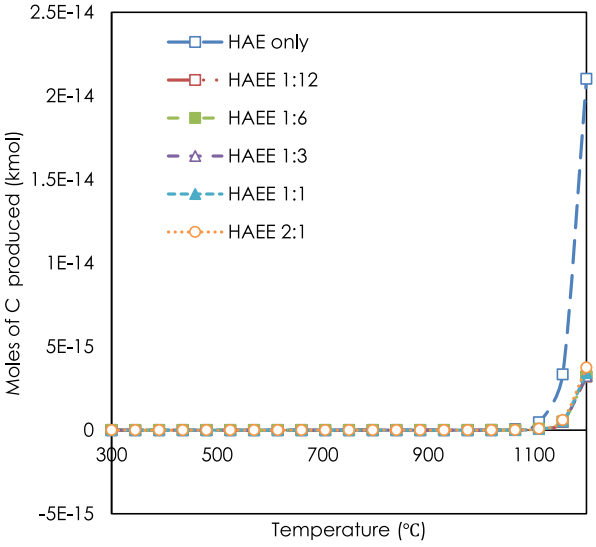

Fig. 19. Yield of C for different HAEE at 1 bar.

Data availability

The data that has been used is confidential.

Acknowledgement

The financial support received from the Ministry of Higher Education Malaysia (MOHE) through the Fundamental Research Grant Scheme (FRGS/1/2020/TK0/UTM/02/97) and Universiti Teknologi Malaysia's Fundamental Research Grant (20H92) is highly appreciated and acknowledged.

References

Aziz, F.H.A., Jusoh, M., Zakaria, Z.Y., 2021. Thermodynamic analysis of hydroxypropanone as bio-oil model compound to light hydrocarbons. Chem. Eng. Transact. 89, 433–438. https://doi.org/10.3303/CET2189073.

Bertero, M., de la Puente, G., Sedran, U., 2012. Fuels from bio-oils: bio-oil production from different residual sources, characterization and thermal conditioning. Fuel 95, 263–271. https://doi.org/10.1016/j.fuel.2011.08.041.

Dhanala, V., Maity, S.K., Shee, D., 2015. Oxidative steam reforming of isobutanol over Ni/γ-Al_2O_3 catalysts: a comparison with thermodynamic equilibrium analysis. J. Ind. Eng. Chem. 27, 153–163. https://doi.org/10.1016/j.jiec.2014.12.029.

Hu, X., Gholizadeh, M., 2020. Progress of the applications of bio-oil. Renew. Sustain. Energy Rev. 134, 110124 https://doi.org/10.1016/j.rser.2020.110124.

Huang, H.-j., Yuan, X.-z., Zhu, H.-n., Li, H., Liu, Y., Wang, X.-l., Zeng, G.-m., 2013. Comparative studies of thermochemical liquefaction characteristics of microalgae, lignocellulosic biomass and sewage sludge. Energy 56, 52–60.

Kumar, R., Strezov, V., Weldekidan, H., He, J., Singh, S., Kan, T., Dastjerdi, B., 2020. Lignocellulose biomass pyrolysis for bio-oil production: a review of biomass pre-treatment methods for production of drop-in fuels. Renew. Sustain. Energy Rev. 123, 109763 https://doi.org/10.1016/j.rser.2020.109763.

Lawal, A., Farrauto, R.J., 2013. Chapter 8 - the convergence of emission control and source of clean energy. In: Suib, S.L. (Ed.), New and Future Developments in Catalysis. Elsevier, Amsterdam, pp. 195–231.

Lehto, J., Oasmaa, A., Solantausta, Y., Kytö, M., Chiaramonti, D., 2018. Fuel oil quality and combustion of fast pyrolysis bio-oils. VTT Technol. 87 https://doi.org/10.13140/RG.2.2.15925.99042.

Liang, L.J., Mohamed, M., Ngadi, N., Jusoh, M., Zakaria, Z.Y., 2021. Thermodynamic analysis of light hydrocarbon production from bio-oil model compound through Co-cracking. In: Proceedings of the 3rd International Conference on Separation Technology Pp 165–174. Lecture Notes in Mechanical – Engineering book series (LNME).

Liu, L., Li, Y., Cui, Y., Fang, S., Wang, K., Chen, J., Li, H., 2019. Thermodynamic analysis on hydrogenation process of phenol of bio-oil model compound. IOP Conf. Ser. Earth Environ. Sci. 310, 042007 https://doi.org/10.1088/1755-1315/310/4/042007.

Londoño-Pulgarin, D., Cardona-Montoya, G., Restrepo, J.C., Muñoz-Leiva, F., 2021. Fossil or bioenergy? Global fuel market trends. Renew. Sustain. Energy Rev. 143, 110905 https://doi.org/10.1016/j.rser.2021.110905.

Ritchie, H., Roser, M., 2020. Energy. Our World in Data.

Rodrigues, C.T., Alonso, C.G., Machado, G.D., de Souza, T.L., 2020. Optimization of bio-oil steam reforming process by thermodynamic analysis. Int. J. Hydrogen Energy 45 (53), 28350–28360. https://doi.org/10.1016/j.ijhydene.2020.07.206.

Sahebdelfar, S., 2017. Steam reforming of propionic acid: thermodynamic analysis of a model compound for hydrogen production from bio-oil. Int. J. Hydrogen Energy 42 (26), 16386–16395. https://doi.org/10.1016/j.ijhydene.2017.05.108.

Sahebdelfar, S., Ravanchi, M.T., 2017. Deoxygenation of propionic acid: thermodynamic equilibrium analysis of upgrading a bio-oil model compound. Renew. Energy 114, 1113–1122. https://doi.org/10.1016/j.renene.2017.07.100.

Velayuthem, S., Mohamed, M., Jusoh, M., Zakaria, Z.Y., 2021. Thermodynamic analysis of ethyl acetate as bio-oil compound to light hydrocarbons. Chem. Eng. Transact. 89, 451–456. https://doi.org/10.3303/CET2189076.

Wang, S., Cai, Q., Wang, X., Zhang, L., Wang, Y., Luo, Z., 2014. Biogasoline production from the Co-cracking of the distilled fraction of biooil and ethanol. Energy Fuels 28, 115–122. https://doi.org/10.1021/ef4012615.

Wang, S., Cai, Q., Chen, J., Zhang, L., Zhu, L., Luo, Z., 2015. Co-cracking of bio-oil model compound mixtures and ethanol over different metal oxide-modified HZSM-5 catalysts. Fuel 160, 534–543. https://doi.org/10.1016/j.fuel.2015.08.011.

Zhang, M., Hu, Y., Wang, H., Li, H., Han, X., Zeng, Y., Xu, C.C., 2021. A review of bio-oil upgrading by catalytic hydrotreatment: advances, challenges, and prospects. Mol. Catal. 504, 111438 https://doi.org/10.1016/j.mcat.2021.111438.